Optics Letters

Intensity noise suppression of a high-power single-frequency CW laser by controlling the stimulated emission rate

Yongrui Guo,[1] Huadong Lu,[1,2,*] Weina Peng,[1] Jing Su,[1,2] and Kunchi Peng[1,2]

[1]State Key Laboratory of Quantum Optics and Quantum Optics Devices, Institute of Optoelectronics, Shanxi University, Taiyuan 030006, China
[2]Collaborative Innovation Center of Extreme Optics, Shanxi University, Taiyuan, Shanxi 030006, China
*Corresponding author: luhuadong@sxu.edu.cn

Received 10 October 2019; accepted 3 November 2019; posted 6 November 2019 (Doc. ID 379744); published 10 December 2019

The intensity noise of a high-power single-frequency continuous-wave (CW) laser is very harmful for applications in precise measurements and quantum communication. By simply lengthening the length of a laser resonator to decrease the stimulated emission rate of the laser, the coupling strength of all noise sources in the resonant laser field will be reduced, and thus the intensity noise of the output laser will be prominently suppressed. Based on theoretical analyses of the laser noise spectra, we experimentally implement a low-noise high-power single-frequency laser with a 1050 mm long resonator. With the assistance of an intracavity imaging system and nonlinear second-harmonic generation, the amplitude of the resonant relaxation oscillation peak and the shot-noise level (SNL) cutoff frequency are successfully reduced to 8.6 dB/Hz above SNL and 1.0 MHz, respectively, under the output power of 16 W. The work provides an effective way to develop a high-quality laser with high output power and low intensity noise. © 2019 Optical Society of America

https://doi.org/10.1364/OL.44.006033

The laser-diode (LD) end-pumped solid-state single-frequency continuous-wave (CW) laser has been widely applied in fields of quantum optics and quantum information, atom cooling and trapping, gravitational wave detection, etc., for its excellent performance, including perfect beam quality, high stability, and low intensity noise. Especially, when the single-frequency CW laser is used as the pump source of high-level entangled or squeezed lights, it is desirable that the cutoff frequency of the intensity noise for the laser is as low as possible, since the entanglement or squeezing level is inversely proportional to the frequency. Unfortunately, the cutoff frequency of the intensity noise for a solid-state single-frequency CW laser is often higher than 3 MHz, which means it is tens of dB higher in intensity noise than the shot-noise limit at ranges lower than 3 MHz for a single-frequency laser, which directly influences the produced squeezing and entanglement levels. Therefore, the high-level squeezed lights have been achieved only at a Fourier analysis frequency higher than 3 MHz [1] so far. If the intensity noise of a laser reaches the shot-noise limit at a frequency of 1 MHz, one can employ it to achieve high-level squeezed light at this frequency band. Thus, it is quite significant to study how to suppress the intensity noise of lasers with a simpler and efficient scheme. Up to date, lots of methods including injection locking, electric-optical feedback controlling, employing a mode cleaner or cascade mode cleaners, self-injection locking, and so on, have been developed. However, a common feature of all these methods is that they are implemented by means of external auxiliary devices, which will inevitably introduce side effects such as complicating laser systems, increasing the cost, introducing additional noise, causing nonnegligible laser power loss, and restricting the output power. Although the intensity noise of a high-power single-frequency laser can be manipulated by inserting a locked electronic-optical etalon into the resonator, the modulation signal for etalon locking still brings additional noise to the laser. Recently, second-harmonic generation (SHG) was used to effectively suppress intensity noise and achieve stable single-longitudinal-mode operation of the laser [2], in which the laser noise around the resonant relaxation oscillation (RRO) frequency was reduced. It is highly desirable to devise an approach that can effectively suppress the intensity noise of high-power single-frequency lasers in a broadband frequency range without additional side effects. In this Letter, we present an efficient and simple scheme to suppress the laser noise without using any additional elements. We theoretically and experimentally demonstrate that not only the linewidth of the laser can be narrowed but also the intensity noise of the laser can be reduced by simply increasing the length of the laser resonator. This is because the high stimulated emission rate (SER) in a laser with a short resonator enhances the coupling strength of all noise sources in the resonant laser field, and thus the noise in the output laser increases. When the length of the resonator is increased, the SER is decreased, which results in the reduction in laser noise.

For a single-frequency CW laser, owing to the interaction between the active atoms and resonant modes of the laser, various noise sources including intensity noise of the pump source, spontaneous emission noise, dipole fluctuations, intensity noise from intracavity losses, and vacuum fluctuations coupled from the output coupler can be introduced into laser systems. Especially, due to population inversions and the damp of the

upper energy level of atoms as well as the intracavity photons, a RRO exists in laser systems. Ralph *et al.* [3] pointed out that the RRO was driven by vacuum fluctuations, dipole fluctuations, spontaneous emission, and intracavity losses, but the intensity noises below and above the frequency of RRO were determined by the pump noise of LD and the vacuum fluctuations, respectively. The intensity noise spectrum of a single-frequency laser can be given by [3]

$$V_f = k_1(\omega_f, \gamma_f) V_{\text{vac}} + k_2(\omega_f, \gamma_f) V_p + k_3(\omega_f, \gamma_f) V_{\text{spont}} + k_4(\omega_f, \gamma_f) V_{\text{dipole}} + k_5(\omega_f, \gamma_f) V_{\text{losses}}, \tag{1}$$

where k_1, k_2, k_3, k_4, and k_5 are the coefficients with respect to the vacuum noise V_{vac} caused by the output coupler; V_{losses}, the noise induced by the intracavity losses; V_p, the noise coming from the pump source; V_{spont}, the noise coming from spontaneous emission; and V_{dipole}, the noise caused by dipole fluctuations, respectively. The RRO frequency ω_f and the damping rate γ_f of the oscillation for V_f are respectively expressed by

$$\omega_f = \sqrt{2\kappa G\alpha^2} \tag{2}$$

and

$$\gamma_f = G\alpha^2 + \Gamma + \gamma_t, \tag{3}$$

where 2κ is the total photon decay rate, which is expressed by $2\kappa = 2\kappa_m + 2\kappa_l . 2\kappa_m = Tc/L$, and $2\kappa_l = \delta c/L$ are the photon decay rates induced by the output losses and the intracavity losses, respectively, where T is the transmission of the output coupling mirror, $\delta = 4.5\%$ is the intracavity linear loss, and c is the velocity of light. Γ is the pump rate [4], and γ_t is the atomic spontaneous emission rate from upper level to lower level. α^2 expresses the intracavity photon number [3]. When the pump rate of the laser Γ is given, ω_f and γ_f depend only on the SER G of the laser. According to Ref. [4], G equals

$$G = \frac{\sigma_s \rho l}{nL}. \tag{4}$$

From Eq. (4), we can see that the SER G is proportional to the stimulated emission cross section σ_s, laser crystal length l, and atomic density ρ, and is inversely proportional to the length L of the resonator and refractive index n of the laser crystal. Substituting Eq. (4) into Eqs. (1)–(3), the relationship between the intensity noise spectrum of the laser and the SER G is attained, which is illustrated in Fig. 1(a), where $V_{\text{vac}} = V_{\text{spont}} = V_{\text{dipole}} = V_{\text{losses}} = 1$ [3], and V_p depends on the intensity noise of the pump field, which is 7 dB above the shot-noise level (SNL) at the pump power of 45 W for the LD of 808 nm wavelength. In Fig. 1(a), we can see that the RRO peak shifts from 680 kHz to 274 kHz when the SER G changes from 5.90×10^{10} s^{-1} to 0.80×10^{10} s^{-1}, and the amplitude of the RRO peak decreases from 43.49 dB/Hz to 34.49 dB/Hz above the SNL. The RRO peak of the laser moves toward the low-frequency direction, and the amplitude of the RRO peak reduces gradually along with the decrease in SER G, which ascribes to a weakened coupling dynamics between the population inversion and intracavity photons. The SNL cutoff frequency also shifts to the low-frequency direction when SER G is decreased. Additionally, lengthening the length L of the laser resonator, the damping rate $2\kappa_m$ is decreased,

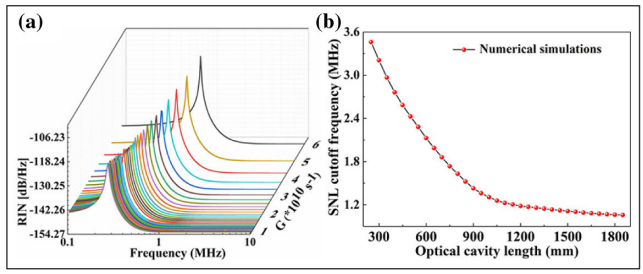


Fig. 1. (a) Numerical simulations of the intensity noise spectra of the laser with different SER G. (b) Theoretical prediction of the SNL cutoff frequency versus length L of resonator.

which weakens the contribution of vacuum fluctuations to the intensity noise at a frequency range higher than the RRO peak. Meanwhile, the photon lifetime within the resonator $\tau_c = 1/(2\kappa)$ increases, and thus the quality factor $Q = 2\pi\nu\tau_c$ of the laser also increases, which results in the enhancement of the ability of resonator filtering nonlasing modes and suppression of intensity noise. It is obvious from Eq. (4) that for a given laser medium, G depends only on L, and thus we can simply manipulate G by changing L. In Fig. 1(a), we obtain the dependence of the SNL cutoff frequency to L, which is depicted in Fig. 1(b). It shows that the SNL cutoff frequency shifts from 3.46 MHz to 1.30 MHz when L is lengthened from 250 mm to 1000 mm. After L is larger than 1000 mm, the change in the cutoff frequency is quite slow, and thus the influence of further increasing L on laser noise will become very small.

From the above theoretical analyses, the length of the laser resonator should be longer than 1000 mm to reduce the noise of the output laser without using complex loss elements and adding any side effects. However, to achieve high output power of the laser, the mode matching between the pump light and the generated laser, the optical conversion efficiency of the laser, and the working stable range (WSR) restricted by the thermal lens effect of the laser crystal have to be carefully considered. Experimentally, we design a single-frequency CW laser with a resonator length of 1050 mm. At first, the WSR for a laser of $L = 1050$ mm as a function of the incident pump power is numerically simulated with an ABCD matrix formalism, shown in Fig. 2(a). It can be seen that the maximum incident pump power of the laser in the WSR is limited to 35 W, and the laser beam waist size is about 770 μm in the center of the laser crystal with respect to a pump-to-mode-size ratio of 0.68. In this case, it is very difficult to obtain high output power of the laser with perfect beam quality because of the limited pump power and poor mode matching together with severe thermal aberration and diffraction loss resulting from a large beam radius of the fundamental mode in the laser crystal. Based on our previous experience in designing a high-power single-frequency CW laser [2], a resonator length of about 400 ∼ 500 mm can well satisfy these design requirements. Figure 2(b) depicts the WSR of the laser with $L = 450$ mm as a function of the incident pump power. It shows that the laser can operate at the WSR under a pump power of 45 W. The beam waist size is about 380 μm in the center of the laser crystal with respect to a pump-to-mode-size ratio of 1.39, which satisfies the mode-matching condition presented by Chen [5]. To achieve the expected WSR and pump-to-mode-size ratio for the laser with $L = 1050$ mm, an imaging system (IS) with negligible optical loss is inserted

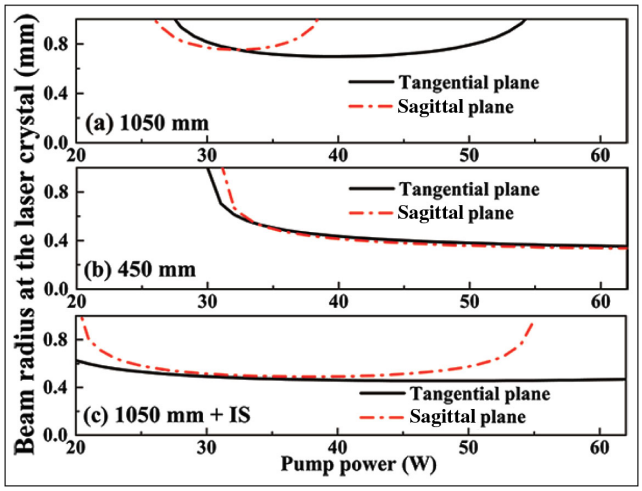


Fig. 2. Working stability range of laser resonator: (a) $L=$ 1050 mm, (b) $L=450$ mm, and (c) $L=1050$ mm including an IS.

in the resonator to change its WSR. The IS is composed of three identical plane–concave lenses with the focal length of 100 mm. The relationships between the WSR of the laser, the distance between the imaging lenses, and the focal length of the thermal lens of the laser crystal are numerically simulated by using ABCD matrix formalism, illustrated in Fig. 2(c). We found that the WSR of the laser is extended to the pump range of 45 W, where the optical distances between the main plane of the laser crystal and f_3, between f_3 and f_4, as well as between f_4 and f_5 are set to 100 mm, 100 mm, and 120 mm, respectively. The beam waist size in the center of the laser crystal is about 500 μm with respect to a pump-to-mode-size ratio of 1.07, which satisfies the mode-matching condition. Besides the laser crystal, a type-I non-critically phase-matched lithium triborate (LBO) crystal (S1, S2: $AR_{1064\ nm;532\ nm}$) with dimensions of 3 mm × 3 mm × 18 mm is inserted into the resonator to effectively suppress the oscillation of the nonlasing modes [2]. The centers of the laser crystal and LBO are precisely placed in the two beam waists of about 500 μm and 70 μm, respectively.

The schematic diagram of the designed laser with $L=1050$ mm and IS system is depicted in Fig. 3. The laser resonator is a bow-tie structure composed of four mirrors M_1-M_4, where M_1 and M_2 are two concave–convex mirrors with curvature radii of $R=1500$ mm, and M_3 and M_4 are two plane–concave mirrors with a curvature radius of $R=-100$ mm. The input coupling mirror M_1 is coated with high-transmissivity (HT) films at 808 nm ($T_{808\ nm}>99.5\%$) and high-reflection (HR) films at 1064 nm ($R_{1064\ nm}>99.7\%$). Both M_2 and M_3 are coated with HR films at 1064 nm ($R_{1064\ nm}>99.7\%$). The output coupling mirror M_4 is coated with the transmission of $T_{1064\ nm}=20\%$ and HT films at 532 nm ($T_{532\ nm}>99.5\%$). The pump source is an 808 nm fiber-coupled LD with the delivering power of 45 W. The core diameter and numerical aperture of the coupling fiber are 400 μm and 0.22, respectively. The pump radiation is focused to be about a 1060 μm diameter spot and injected at the center of the laser crystal. The laser crystal is an a-cut composite $YVO_4/Nd:YVO_4$ rod (S1, S2: $AR_{808\ nm;1064\ nm}$) with an un-doped end cap of 5 mm and a 0.2 at. % Nd-doped part of 15 mm. A small angle of 1.5° is cut at the rear end-face of

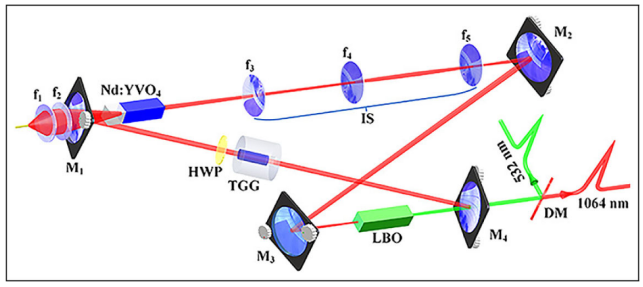


Fig. 3. Schematic of the experimental setup. TGG, terbium gallium garnet; LBO, lithium triborate; HWP, half-wave plate; f_{1-2}, lens; DM, dichroic mirror; IS, imaging system.

the laser crystal to retain stable polarization of the laser. To eliminate the spatial hole burning effect and achieve unidirectional operation of the laser, an optical diode comprising an 8 mm long terbium gallium garnet crystal and a half-wave plate is employed. The output laser beams of 1064 nm and 532 nm are separated by the dichroic mirror. The longitudinal-mode structures of L_1 and L_2 lasers at 1064 nm are monitored by scanning the confocal Fabry-Perot (F-P) cavity with a free spectral range of 375 MHz and finesse of 180, respectively.

When the temperature of the LBO crystal is set to room temperature, which is far from the optimal phase-matching value, the output powers of the two lasers with resonator lengths of $L_1=450$ mm and $L_2=1050$ mm including an IS system are recorded as a function of the incident pump powers, shown in Fig. 4(a). In Fig. 4(a), we can see that the threshold pump powers as well as the laser output powers under the pump power of 45 W for L_1 (blue) and L_2 (red) lasers are 32.6 W and 32.1 W, as well as 16.4 W and 17.1 W, respectively. The linewidth of L_1 and L_2 lasers under single-frequency operation are measured by employing a delayed self-heterodyne (SHD) interferometer with a path length imbalance of 25 km between long and short branches of the interferometer [2]. The measured SHD linewidth data and the Gaussian lineshape function fitting results are shown in Fig. 4(b), wherein the 3 dB spectral linewidth of the L_2 laser is narrowed from 213 kHz for the L_1 laser to 71 kHz. The intensity noise for L_1 and L_2 lasers is measured by a homemade balanced homodyne detector (BHD, Yuguang Co., Ltd.) with incident laser power of 1 mW. The output signal of the BHD is recorded by a spectrum analyzer (SA) with a resolution bandwidth (RBW) of 30 kHz and video bandwidth (VBW) of 30 Hz. The measured results

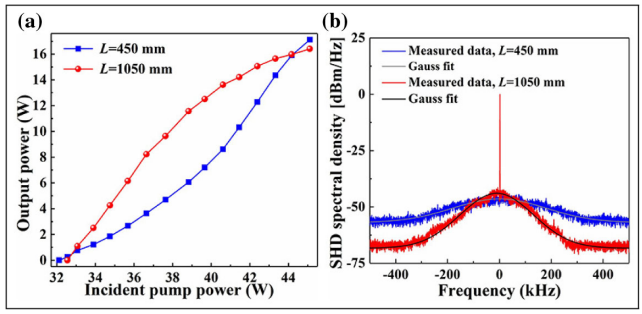


Fig. 4. (a) Output power of the laser with $L=450$ mm and $L=1050$ mm versus incident pump power. (b) Corresponding measured SHD linewidth data with a 25 km delay fiber and Gaussian function fitting results.

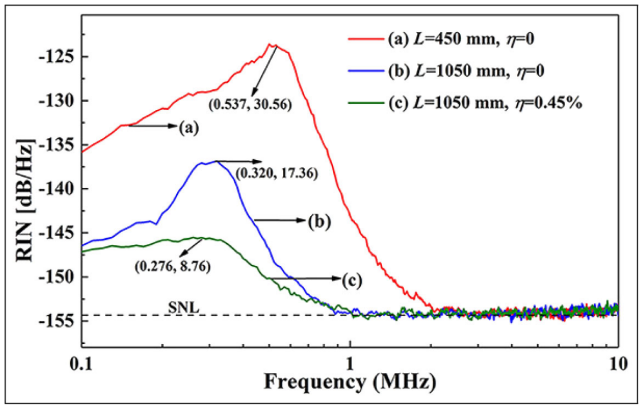


Fig. 5. (a) Measured intensity noise spectra for L_1 laser with $\eta = 0$, (b) L_2 laser with $\eta = 0$, and (c) L_2 laser with $\eta = 0.45\%$.

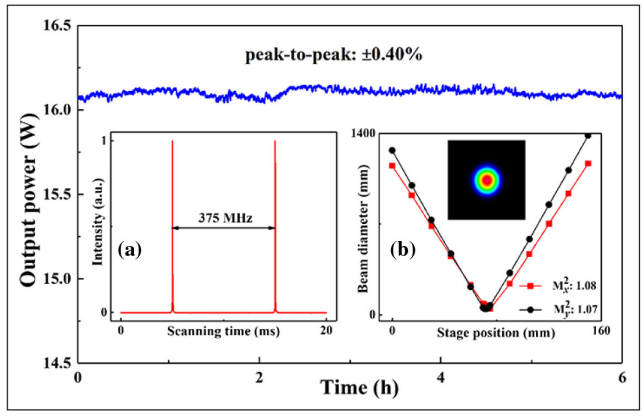


Fig. 6. Power stability for L_2 laser with nonlinear loss. The insets are (a) single-longitudinal-mode structure, and (b) beam quality M^2-factor.

depicted by the relative intensity noise (RIN) are shown in curves (a) and (b) in Fig. 5, respectively. It can be obviously seen that by lengthening the laser resonator length from L_1 to L_2 under the help of the IS, the frequency and amplitude of the RRO peak are decreased from 537 kHz to 320 kHz and from 30.56 dB/Hz to 17.36 dB/Hz above the SNL, respectively. Especially, the lowest SNL cutoff frequency for the L_2 laser has been reduced to 1.0 MHz from 2.6 MHz for the L_1 laser. Although the threshold and output laser powers are almost the same in this operation condition, the noise spectra of the two lasers are different, and the noise spectrum for the L_2 laser is much lower than that for the L_1 laser, just as theoretically expected. The experimental results prove that by lengthening the length of the resonator and adding an appropriate IS in the cavity, the intensity noise of a high-power single-frequency laser can be effectively suppressed. Also, we experimentally demonstrate that the RIN for the L_2 laser around the RRO peak can be further suppressed by using the intracavity SHG, which is implemented by tuning the temperature of the LBO crystal to the optimal phase-matching point of 149°C. Then, the maximum output powers for 1064 nm and 532 nm lasers are measured to be 16.1 W and 0.36 W at a pump power of 45 W, respectively. The RIN spectrum of the laser depicted in curve (c) in Fig. 5 shows that when the nonlinear loss of $\eta = 0.45\%$ [2] is added in the L_2 laser, the frequency and amplitude of the RRO peak are significantly reduced from 320 kHz to 276 kHz and from 17.4 dB/Hz to 8.6 dB/Hz above the SNL, respectively, and the RRO peak nearly disappears. The experimental results reveal that the intensity noise of a single-frequency laser including the RRO peak and the SNL cutoff frequency can be effectively suppressed and decreased by combining the two technologies of manipulating the SER of a laser and utilizing the intracavity SHG. Last, other parameters of the L_2 laser are also measured in the experiment. Figure 6 depicts the power stability of the L_2 laser at an output power of 16.1 W, where the peak-to-peak power stability during 6 h is better than ±0.40%. The inset in Fig. 6(a) shows the longitudinal-mode structure of the L_2 laser, which reveals that the laser can work with stable single frequency with the assistance of nonlinear loss. The inset in Fig. 6(b) depicts the measured beam quality of the laser (M2SETVIS, Thorlabs), and the measured values of M_x^2 and M_y^2 are 1.08 and 1.07, respectively.

In conclusion, we develop an effective method to suppress the intensity noise of a high-power single-frequency CW laser by controlling the SER of a laser. We theoretically and experimentally demonstrate that by simply lengthening the length of the resonator to decrease the SER of a laser, the intensity noise of the laser can be effectively suppressed. When the SER of a high-power single-frequency laser is decreased from $G_1 = 3.28 \times 10^{10}\text{s}^{-1}$ to $G_2 = 1.40 \times 10^{10}\text{s}^{-1}$ by lengthening the laser resonator length from $L_1 = 450$ mm to $L_2 = 1050$ mm with the assistance of an IS and the intracavity SHG, the frequency and amplitude of the RRO peak are significantly reduced from 537 kHz to 276 kHz and from 30.56 dB/Hz to 8.76 dB/Hz above the SNL, respectively. Especially, the lowest SNL cutoff frequency for the L_2 laser is reduced to 1.0 MHz from 2.6 MHz for the L_1 laser, and the laser linewidth is also narrowed to 71 kHz from 211 kHz. The experimental results agree well with theoretical predictions. Although the experimental comparison is implemented in two specific single-frequency solid lasers, the presented scheme can be applied to other lasers with higher output powers. We believe that the proposed method for reducing intensity noise of lasers will provide a useful technical reference for the design of high-quality lasers.

Funding. Key Project of the Ministry of Science and Technology of the People's Republic of China (2017YFB0405203).

Disclosures. The authors declare no conflicts of interest.

REFERENCES

1. H. Vahlbruch, M. Mehmet, K. Danzmann, and R. Schnabel, Phys. Rev. Lett. **117**, 110801 (2016).
2. Y. R. Guo, H. D. Lu, M. Z. Xu, J. Su, and K. C. Peng, Opt. Express **26**, 21108 (2018).
3. C. C. Harb, T. C. Ralph, E. H. Huntington, D. E. McClelland, and H. A. Bachor, J. Opt. Soc. Am. B **14**, 2936 (1997).
4. J. Zhang, K. S. Zhang, Y. L. Chen, T. C. Zhang, C. D. Xie, and K. C. Peng, Acta Opt. Sinica **20**, 1311 (2000).
5. Y. F. Chen, J. Opt. Soc. Am. B **17**, 1835 (2000).